JOC Article

Synthetic Model of the Phosphate Binding Protein: Solid-State Structure and Solution-Phase Anion Binding Properties of a Large Oligopyrrolic Macrocycle

Evgeny A. Katayev,*,† Jonathan L. Sessler,*,‡ Victor N. Khrustalev,† and Yuri A. Ustynyuk§

A. N. Nesmeyanov Institute of Organoelement Compounds, Russian Academy of Sciences, 28, Vavilov Street, 119991, Moscow, Russian Federation, Department of Chemistry and Biochemistry and Institute for Cellular and Molecular Biology, 1 University Station-A5300, University of Texas at Austin, Austin, Texas 78712-0165, and Department of Chemistry, M. V. Lomonosov Moscow State University, Leninskie Gory, 119992 Moscow, Russian Federation

katayev@ineos.ac.ru; sessler@mail.utexas.edu

Received May 31, 2007

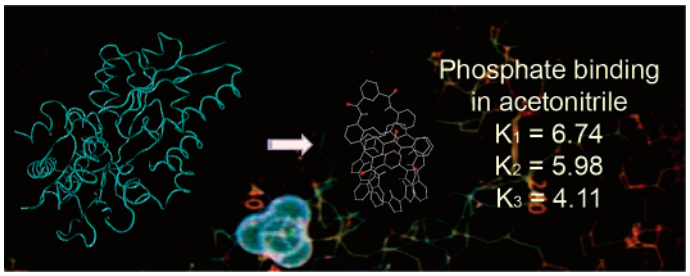

The macrocyclic receptors **4**−**6** were synthesized via the anion-templated condensation of appropriately chosen dialdehyde and diamine building blocks. Whereas all three products could be obtained directly via the appropriate choice of reaction conditions, the larger [3+3] product, **6**, which incorporates three of each precursor subunit, could also be obtained conveniently via an indirect procedure involving ring expansion of the smaller [2+2] macrocycle **4**. As detailed earlier (Sessler, J. L.; Katayev, E. A.; Pantos, G. D.; Reshetova, M. D.; Khrustalev, V. N.; Lynch, V. M.; Ustynyuk, Y. A. *Angew. Chem.* **2005**, *117*, 7552−7556; *Angew. Chem., Int. Ed.* **2005**, *44*, 7386−7390), this ring expansion occurs under thermodynamic control in the presence of HSO_4^- and $H_2PO_4^-$ anions in acetonitrile solution and serves to effect the conversion of **4** to **6**. An analysis of the X-ray crystal structure of complex $\mathbf{6}H_2^{2+}\cdot HPO_4^{2-}$ revealed a strong resemblance to the active site of the phosphate binding protein (PBP) with similar structural analogies being drawn between the active site of the sulfate binding protein (SBP) and the corresponding hydrogensulfate anion complex. In both cases, the anions are bound in a 1:1 fashion in the solid state through a complementary hydrogen bond network involving both the receptor **6** and the anions. UV−vis spectroscopic titrations provide support for the conclusion that macrocycle **6** binds the hydrogensulfate and dihydrogenphosphate anion (studied as the corresponding tetrabutylammonium salts) with high selectivity and affinity in acetonitrile (log K_a for the first binding interaction approaching 7), albeit with different receptor-to-anion binding stoichiometries (1:1 vs 1:3 for HSO_4^- and $H_2PO_4^-$, respectively).

Introduction

Ever since the anion recognition properties of simple organic molecules were noted more than 30 years ago, considerable effort has been devoted to the synthesis of anion receptors and sensors.[1] The anion−host interaction principles elucidated in the course of these studies have served to animate advances in such disparate areas as sensor technology,[2] waste remediation,[3] catalysis, and drug discovery.[4,5] Meanwhile, a specific objective

† Russian Academy of Science.
‡ University of Texas at Austin.
§ M. V. Lomonosov Moscow State University.

(1) Sessler, J. L.; Gale, P. A.; Cho, W.-S. *Anion Receptor Chemistry*; Royal Society of Chemistry: Letchworth, UK, 2006.
(2) Beer, P. D.; Gale, P. A. *Angew. Chem., Int. Ed.* **2001**, *40*, 486−516.

10.1021/jo071106g CCC: $37.00
Published on Web 08/18/2007

has been to develop receptors that can mimic the anion recognition motifs found in natural systems,[6] including the phosphate- and sulfate-binding proteins (PBP and SBP), protein kinases, and phosphatases. This is because an increased understanding of the underlying anion recognition features exploited by Nature is expected to lead to improvements in structure-based drug design, as well as better modeling of the natural enzymatic processes.[7] Recently we reported the synthesis of receptors induced by using the conjugate acid of a specifically targeted anion as a template for macrocycle formation. Two phosphate selective receptors **1**[8] and **4**[9] were prepared in this way and were shown to possess binding affinities of up to log $K_a = 5$ in acetonitrile for the first binding event with an overall 1:2 (receptor to dihydrogenphosphate anion) binding stoichiometry. In this paper we report a template-mediated synthesis of the larger system **6** and a detailed analysis of the hydrogen-bonding networks present in its phosphoric acid and sulfuric acid salts. We also report the first synthesis of a reduced analogue of **4** (macrocycle **5**), efforts to produce the smaller congeners **2** and **3**, as well as solution phase anion binding studies involving all three larger bipyrrole-containing receptors (**4**−**6**). On the basis of the structural similarity (cf. Table 1) between the phosphoric acid salt **6**·H_3PO_4, which is seen to be the dihydrogenphosphate complex, $\mathbf{6}H_2^{2+}\cdot HPO_4^{2-}$ in the solid state, and the binding site seen in the PBP,[5, 10, 11] as well as the recognized ability of its free base form to bind phosphate anions in acetonitrile solution, we conclude that receptor **6** may be considered as a rudimentary synthetic model for this naturally occurring anion binding protein.

Results and Discussion

General aspects of tetrahedral oxoanion receptors have recently been reviewed by us[6] and others.[12] In the case of phosphate anions, charged polyamine[13] and guanidine[14] receptors, protonated expanded porphyrins,[15] and various zinc- and copper-based complexes[16] have proved to be the most efficient systems. In recent studies we have found that appropriately designed pyrrole−pyridine hybrid macrocycles show promise as phosphate anion receptors.[8,17] These systems, built up from pyrrolic and amidopyridine precursors, were designed to incorporate both H-donor and acceptor sites within the same overall receptor framework. This strategy, which provides a complement to the recent work of Bowman-James[18] and Gale,[19] was inspired by the specific challenge of creating a synthetic model for the active center of PBP. However, in contrast to the approach adopted by others, in our case imine bonds, rather than the amide functionality, were used to link the various "building blocks". This was done so as to build on our previous efforts in the expanded porphyrin area and to produce systems that are potentially amenable to acid-catalyzed, template-mediated formation. This choice was also expected to produce macrocyclic products that contain ancillary H-bond acceptor sites. Since inorganic phosphate and its derivatives can exist in several protonated forms (e.g., $H_2PO_4^-$ and HPO_4^{2-}) at or near physiological pH, it was specifically thought that the use of imine linkers, which might be subject to protonation, would allow for the accommodation of these different forms.

In this work, 3,3′-dimethyl-4,4′-dipropyl-5,5′-diformyl-2,2′-bipyrrole **7** and the diamine building blocks **8** and **9** were used to produce the small combinatorial library of receptors **2**−**6** (Figure 1). The selection of ostensibly similar amide (**8**)- and amine (**9**)-linked *o*-phenylenediamine-derived precursors was made so as to be able to assess the importance of the putative H-bond acceptor binding sites in the resulting receptors (i.e., through use of the aminomethyl precursor, **9**, and amide precursor, **8**, respectively).[20] Since these precursors also differ in their inherent rigidity, we were likewise curious to see if their use would give rise to different ratios of combinatorial products (e.g., [1+1], [2+2], [3+3], etc.) incorporating different numbers of precursor subunits, under otherwise identical ring-forming conditions.

As in the case of our previous studies, acid-promoted imine formation was chosen to effect macrocyclization. Under the conditions employed (precursor concentrations of ca. 0.1−0.15 M; 2 molar equiv of acid; methanol as solvent), this reaction is inherently reversible, and was thus expected to depend not only on the choice of precursor but also on the choice of acid catalyst. In accord with such expectations, initial screening studies revealed that only phosphoric and sulfuric acids gave rise to the larger macrocyclic products **4**−**6** in good yields. The use of other acids, including HCl, HBr, CF_3COOH, HNO_3, $HClO_4$, and $HReO_4$, gave rise to mixtures of products **2**−**6** as deduced from MALDI-TOF or ESI mass spectrometric analysis. On the basis of these findings, we infer that phosphoric and sulfuric acid work well as templates for the clean formation of **4**−**6** because the corresponding conjugate anions fit well within the hydrogen-bonding network provided by the incipient macrocyclic receptor. Within the context of this overall conclusion, it is of interest to note that the use of sulfuric acid in the reaction of building blocks **7** and **8** leads to the formation of the bis-sulfuric acid salt of **4** (the [2+2] condensation product) in almost 90% yield, whereas the use of phosphoric acid leads to the formation of the monophosphoric salt of macrocycle **6** (the [3+3] product) in 46% yield (Scheme 1). Interestingly, the [1+1] product, compound **2** (or its protonated derivatives), could

(3) Bianchi, A.; Bowman-James, K.; Garcia-España, E. *Supramolecular Chemistry of Anions*; Wiley-VCH, New York 1997.
(4) Darbre, T.; Reymond, J.-L. *Acc. Chem. Res.* **2006**, *39*, 925−934.
(5) Morales, R.; Berna, A.; Carpentier, P.; Contreras-Martel, C.; Renault, F.; Nicodeme, M.; Chesne-Seck, M. L.; Bernier, F.; Dupuy, J.; Schaeffer, C.; Diemer, H.; Van-Dorsselaer, A.; Fontecilla-Camps, J. C.; Masson, P.; Rochu, D.; Chabriere, E. *Structure* **2006**, *14*, 601−609.
(6) Katayev, E. A.; Ustynyuk, Y. A.; Sessler, J. L. *Coord. Chem. Rev.* **2006**, *250*, 3004−3037.
(7) Hirsch, A. K. H.; Fischer, F. R.; Diederich, F. *Angew. Chem., Int. Ed.* **2007**, *46*, 338−352.
(8) Sessler, J. L.; Katayev, E.; Pantos, G. D.; Ustynyuk, Y. A. *Chem. Commun.* **2004**, 1276−1277.
(9) Katayev, E. A.; Pantos, G. D.; Reshetova, M. D.; Khrustalev, V. N.; Lynch, V. M.; Ustynyuk, Y. A.; Sessler, J. L. *Angew. Chem., Int. Ed.* **2005**, *44*, 7386−7390.
(10) Luecke, H.; Quiocho, F. A. *Nature* **1990**, *347*, 402−406.
(11) Yao, N.; Ledvina, P. S.; Choudhary, A.; Quiocho, F. A. *Biochemisrty* **1996**, *35*, 2079−2085.
(12) Kang, S. O.; Hossain, M. A.; Bowman-James, K. *Coord. Chem. Rev.* **2006**, *250*, 3038−3052.
(13) Llinares, J. M.; Powell, D.; Bowman-James, K. *Coord. Chem. Rev.* **2003**, *240*, 57−75.
(14) Schmidtchen, F. P. *Coord. Chem. Rev.* **2006**, *250*, 2916−2928.
(15) Sessler, J. L.; Davis, J. M. *Acc. Chem. Res.* **2001**, *34*, 989−997.
(16) O'Neil, E. J.; Smith, B. D. *Coord. Chem. Rev.* **2006**, *250*, 3068−3080.
(17) Katayev, E. A.; Boev, N. V.; Khrustalev, V. N.; Ustynyuk, Y. A.; Tananaev, I. G.; Sessler, J. L. *J. Org. Chem.* **2007**, *72*, 2886−2896.
(18) Kang, S. O.; Begum, R. A.; Bowman-James, K. *Angew. Chem., Int. Ed.* **2006**, *45*, 7882−7894.
(19) Brooks, S. J.; Gale, P. A.; Light, M. E. *Supramol. Chem.* **2007**, *19*, 9−15.
(20) Sessler, J. L.; Katayev, E.; Pantos, G. D.; Scherbakov, P.; Reshetova, M. D.; Khrustalev, V. N.; Lynch, V. M.; Ustynyuk, Y. A. *J. Am. Chem. Soc.* **2005**, *127*, 11442−11446.

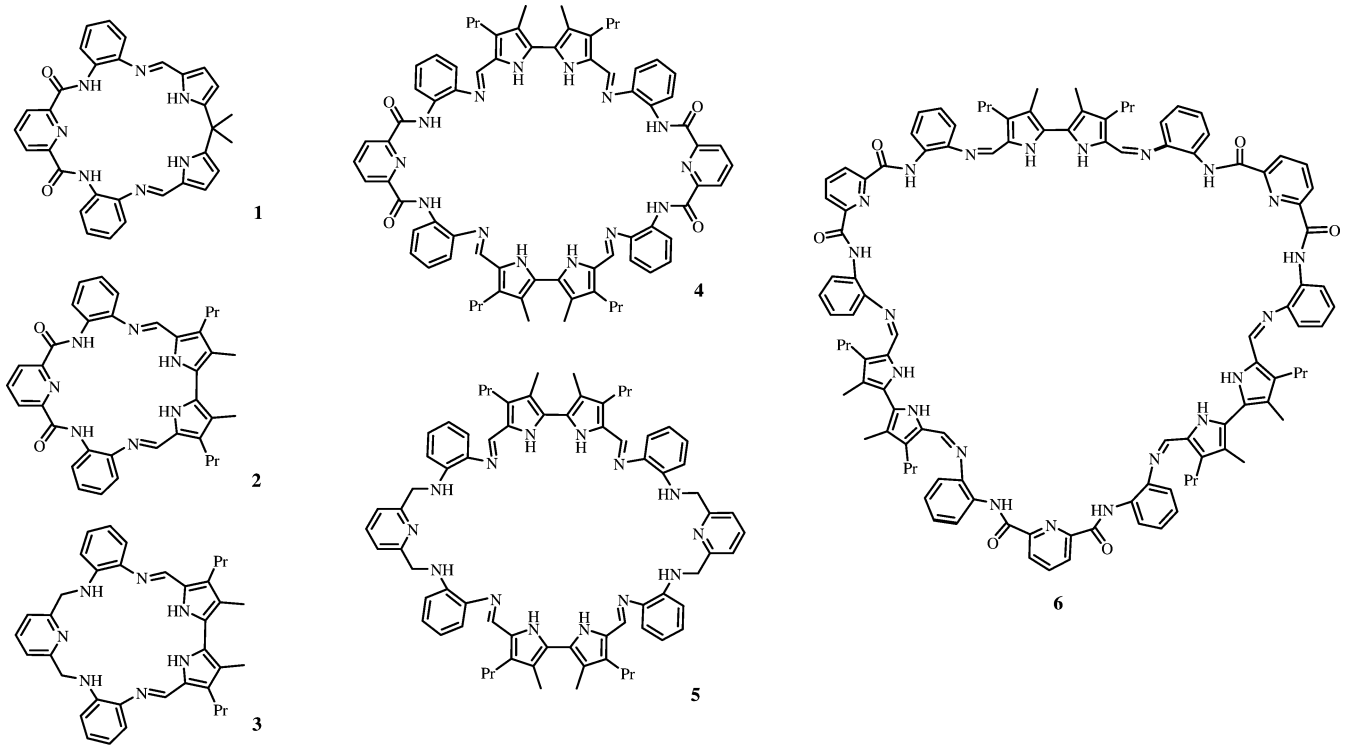

FIGURE 1. Hybrid macrocycles germane to the present study.

SCHEME 1. Products of Sulfuric and Phosphoric Acid Templated Cyclizations of Building Blocks 7−9

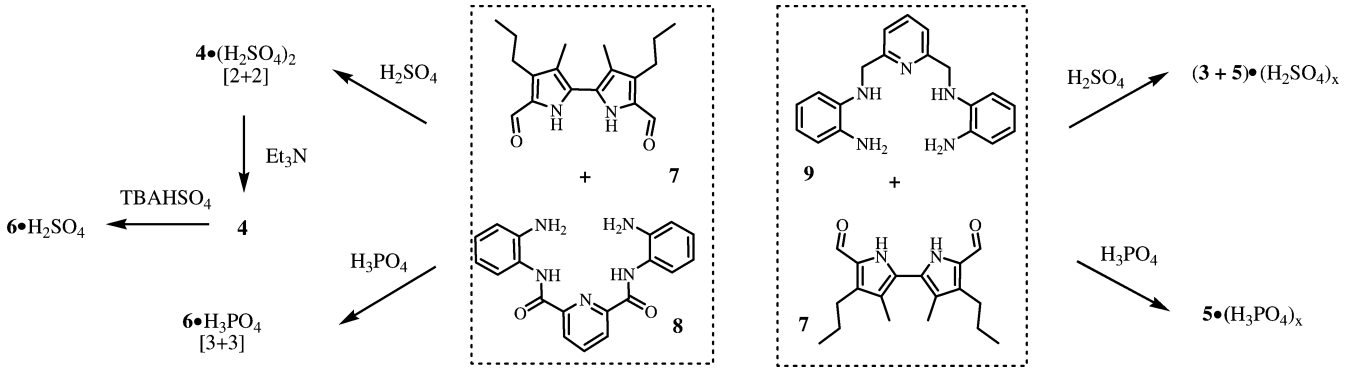

not be obtained in isolable quantities by using either procedure. When the pyridine-2,6-diaminomethyl containing building block **9** was used, the use of phosphoric acid produced the [2+2] product **5** in 72% yield, while sulfuric acid gave rise to a mixture of the acid salts of [1+1] (**3**) and [2+2] (**5**) condensation products (Scheme 1) that did not prove amenable to ready separation. Under neither set of conditions were appreciable quantities of [3+3] product, corresponding to a pyridine-containing analogue of **6** (structure not shown), observed. On this basis it is concluded that both the choice of acid template and the nature of the pyridine-containing precursors are critical to defining the nature of the products produced under the present imine-forming macrocyclization conditions.

Once produced, the free receptors could be obtained via neutralization of the acid salts with an excess of triethylamine in methanol solution. In general, these free-base forms are stable in solution for 2−3 days under normal laboratory conditions or for months in the solid phase. However, when the free receptor form of the [2+2] product **4** was allowed to stand for 5 days in acetonitrile in the presence of hydrogensulfate or dihydrogenphosphate anion (in the form of the corresponding tetrabutylammonium salts), followed by crystallization, the larger [3+3] product **6** was isolated.[9] Although cation-mediated expansions of imine-derived macrocyclic receptors are known, having been studied in some detail recently by Love and co-workers,[21] corresponding anion-mediated ring expansions have only recently been shown to be possible.[9]

No expansion of macrocycle **4** was observed when an excess of ammonium sulfate was used in place of tetrabutylammonium hydrogensulfate, again in acetonitrile solution. On this basis, we conclude that the presence of protons (from, e.g., HSO_4^- or $H_2PO_4^-$) is required to induce what must be a thermodynamically driven reorganization of the receptor via solvolysis of the imino bonds. To the extent such a conclusion is correct, it implies that, at least in acetonitrile, receptor **6** has a higher

(21) Givaja, G.; Blake, A. J.; Wilson, C.; Schroder, M.; Love, J. B. *Chem. Commun.* **2005**, 4423−4425.

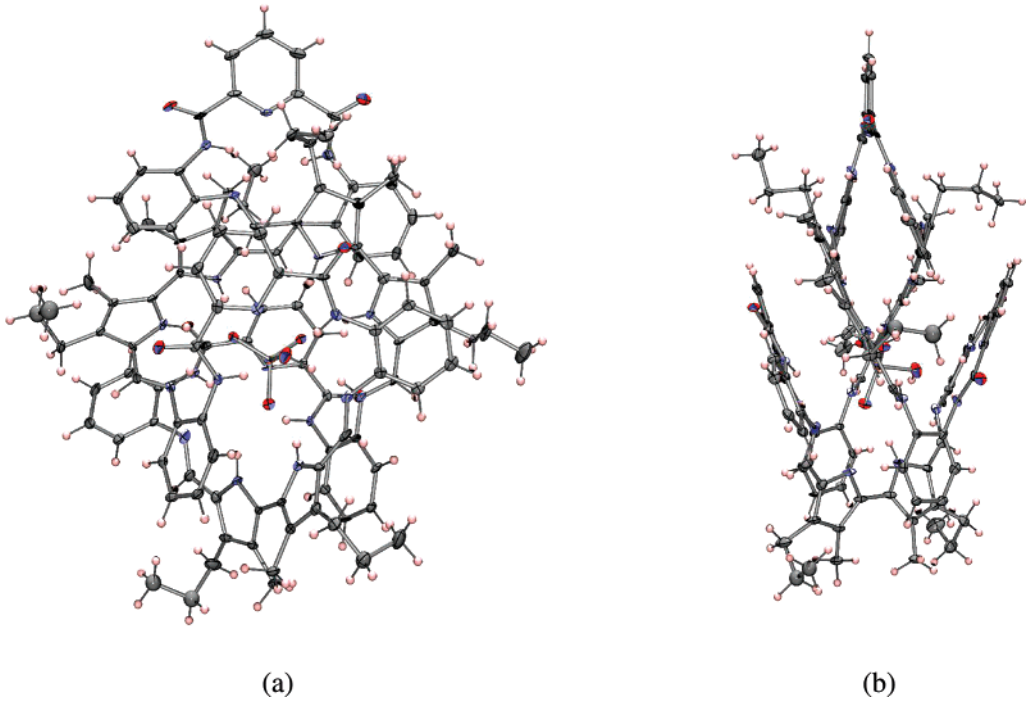

FIGURE 2. ORTEP POV-ray rendering of the structure of **6**·H_3PO_4 as deduced from a single-crystal X-ray diffraction analysis: (a) view along the *c*-axis and (b) view along the *a*-axis. Ellipsoids are shown at the 20% probability level.

affinity for the hydrogensulfate and dihydrogenphosphate anions than does its smaller congener **4**. One of the objectives of the present study was to test the extent to which such a conclusion is correct.

Solid-State Structural Analyses and Comparisons with the Active Sites of the PBP and SPB. Prior to carrying out solution-phase studies, we sought to obtain insights from solid-state structural analyses. Although we succeeded in obtaining diffraction grade crystals for **4** and **6**, unfortunately this success did not translate into the other members of the present series. Macrocycles such as **1**−**6** have proved difficult to crystallize, in part because the acid salts display poor solubility in all common organic solvents and water. Macrocycle **4** was thus crystallized as solvate with 2 molecules of water encapsulated within the figure-8 shaped core, while macrocycle **6** was first crystallized as its sulfuric acid complex, **6**·H_2SO_4, as was discussed by us recently,[9] and now as the phosphoric acid salt in the context of this work. In both structures involving **6**, the solid-state species are best considered as complexes of the corresponding dianion in the solid state (i.e., **6**H_2^{2+}·SO_4^{2-} and **6**H_2^{2+}·HPO_4^{2-}, respectively), as inferred from the overall structure and from the fact that the hydrogen atoms bound to nitrogen and phosphorus atoms were specifically observed in the ΔF map for the new structure of **6**·H_3PO_4. For both structures, which are nearly identical, there are two crystallographically independent molecules in the unit cell, which reflect different conformers. From an inspection of Figure 2, which shows the structure of **6**H_2^{2+}·HPO_4^{2-}, one can see that the large macrocycle is twisted around the anion, forming a tight hydrogen bond network. Three bipyrrole subunits surround the anion. Two of these subunits act as cross sections for the macrocycle, while the other defines the bottom of the receptor (Figure 2b). To the right and left sides of the anion, there are two diamidopyridine subunits that are oriented parallel to the bipyrrole units. From an analysis of the X-ray structural parameters, it is inferred that receptor **6** is doubly twisted in the case of this structure, just as it was in the previous one involving **6**H_2^{2+}·SO_4^{2-}. The P−O distances are different and equal to 1.497(4), 1.500(4), 1.503(4), and 1.625(5) Å (cf. the Experimental Section in the Supporting Information). These distances compare to the corresponding S−O parameters of 1.470(4), 1.475(4), 1.458(4), and 1.459(4) Å seen in the structure of **6**H_2^{2+}·SO_4^{2-} reported earlier.[9]

To facilitate a comparison of the hydrogen bond networks that stabilize[1] the bound anions in the solid structures of **6**·H_3PO_4 and **6**·H_2SO_4 with those present at the active sites of the SBP[22] and PBP,[10] a schematic representation of the respective anion coordination motifs is given in Figure 3. Relevant structural parameters for the hydrogen bonding interactions are given for all four systems in Tables 1 and 2. As can be seen from this drawing and inferred from these tables, in all four structures the average distances between the atoms involved in the hydrogen bonding interactions are very similar to one another and can be considered the same within the error limits. The average angles of the individual hydrogen bonds are slightly smaller for the model systems than for the enzymes, a disparity that is ascribed to the rigidity of the macrocycle. In the synthetic systems a network of hydrogen bond donors and acceptors is established via a combination of three 2-iminobipyrrole subunits, two 2,6-diamidopyridine fragments, and two protonated imine residues per bound anion. In the case of the hydrogenphosphate complex, **6**H_2^{2+}·HPO_4^{2-} (**6**·H_3PO_4), one imine nitrogen acts as a hydrogen bond acceptor and interacts with O(4)H from the anion. In contrast, the other imine interacts with O(3). Thus, the bound hydrogenphosphate anion is stabilized by one more hydrogen bonding interaction than the sulfate anion present in the structure of **6**·H_2SO_4 (12 vs 11). The principle difference between these two structures thus lies in O4 coordination mode

(22) Pffugrath, J. W.; Quiocho, F. A. *Nature* **1985**, *314*, 257−260.

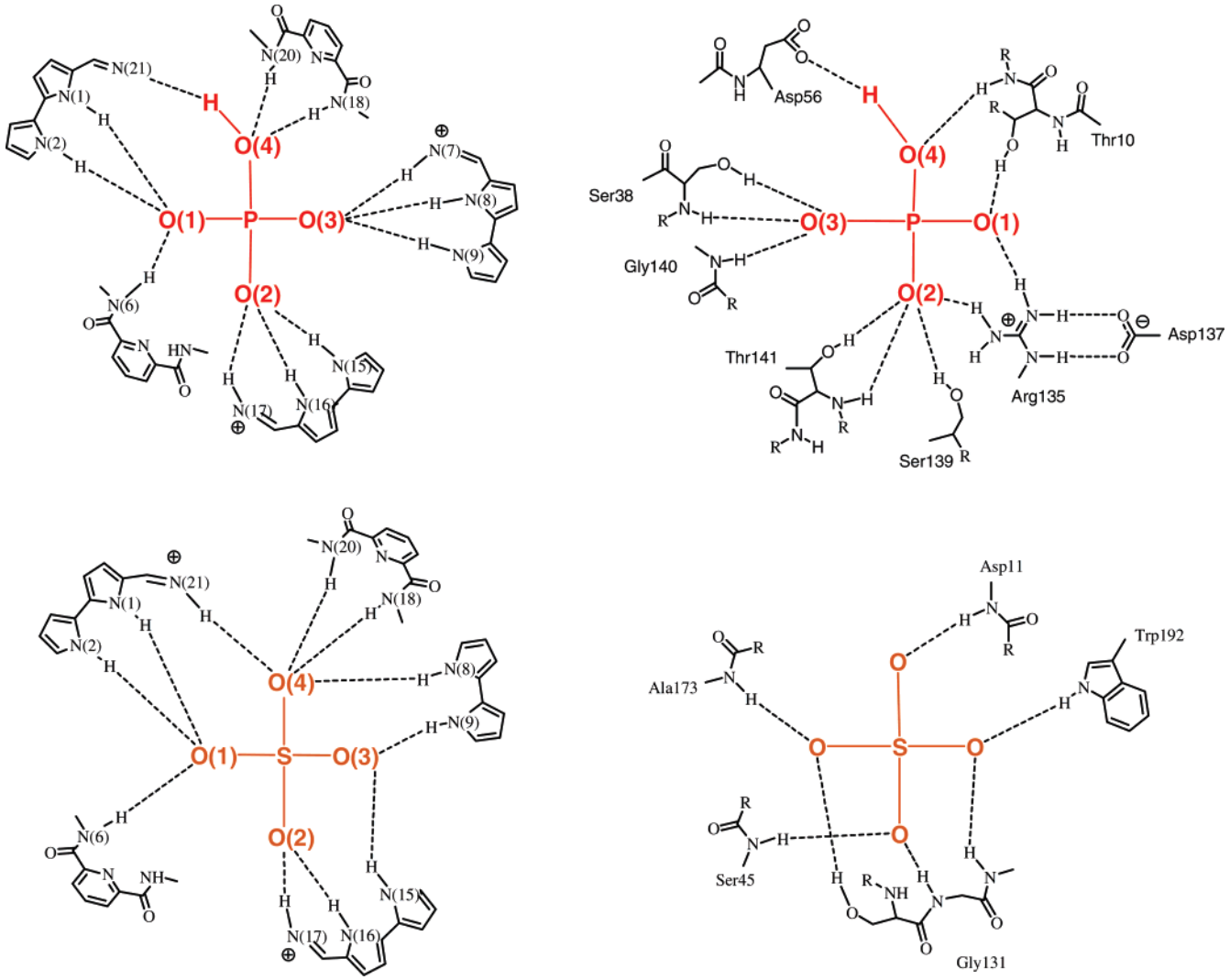

FIGURE 3. Schematic representations of the hydrogen bond networks present in complexes $\mathbf{6}H_2^{2+}\cdot HPO_4^{2-}$ and $\mathbf{6}H_2^{2+}\cdot SO_4^{2-}$ (structures $\mathbf{6}\cdot H_3PO_4$ and $\mathbf{6}\cdot H_2SO_4$, respectively) and the active sites of the PBP and SBP.

TABLE 1. Geometric Parameters Corresponding to the Anion-Stabilizing Hydrogen Bond Interactions in the PBP[10] and $6\cdot H_3PO_4$

PBP				$6\cdot H_3PO_4$			
phosphate atom	Y (atom)	distance (Å) X···Y	angle (deg) X···H···Y	phosphate atom	Y (atom)	distance (Å) X···Y	angle (deg) X···H···Y
O1	NH(Thr10)	2.81	156.0	O1	N1	2.825	156
	OH(Thr10)	2.69	167.2		N2	2.812	148
	NH(Arg135)	2.84	172.3		N6	3.011	107
O2	NH(Arg135)	2.90	148.9	O2	N15	2.947	160
	OH(Ser139)	2.77	169.0		N16	2.714	162
	NH(Thr141)	2.83	159.2		N17	2.936	163
	OH(Thr141)	2.68	149.7				
O3	NH(Ser38)	2.67	163.9	O3	N7	2.799	172
	OH(Ser38)	2.63	160.9		N8	2.714	164
	NH(Gly140)	2.76	177.1		N9	3.337	138
O4	NH(Phe11)	2.92	163.3	O4	N20	2.994	131
	O(Asp56)	2.45	151.2		N18	3.039	143
					N21	2.711	159
	average	2.75	162	average		2.903	150

and in the way the bipyrrole fragment N7−N8−N9 interacts with the anion (Figure 3). Specifically, the imino group N7 is seen to participate in hydrogen binding with the phosphate oxygen, but not with the bound sulfate anion; in this case, nitrogens N8 and N9 are directed to different oxygen atoms, O(4) and O(3). This difference is ascribed to differences in the orientation of the tetrahedral oxyanions relative to the receptor; in $\mathbf{6}\cdot H_3PO_4$ the hydrogenphosphate anion is rotated by 10° in toward O4 → O3 as compared to what is seen in the case of the corresponding sulfate anion complex, $\mathbf{6}H_2^{2+}\cdot SO_4^{2-}$ ($\mathbf{6}\cdot H_2SO_4$).

TABLE 2. Geometric Parameters Corresponding to the Anion-Stabilizing Hydrogen Bond Interactions in the SBP[22] and 6·H_2SO_4

SBP				**6**·H_2SO_4			
sulfate atom	Y (atom)	distance (Å) X···Y	angle (deg) X···H···Y	sulfate atom	Y (atom)	distance (Å) X···Y	angle (deg) X···H···Y
O1	OH(Ser130)	2.76	167	O1	N1	2.986	159
	NH(Ala137)	2.70	151		N2	2.740	148
					N6	2.982	127
O2	NH(Ser45)	2.84	169	O2	N16	2.839	166
	NH(Gly131)	2.83	170		N17	2.923	170
O3	NH(Gly132)	2.77	149	O3	N9	2.938	171
	NH(Trp192)	2.82	157		N15	3.349	145
O4	NH(Asp11)	2.67	152	O4	N8	3.420	159
					N18	3.347	146
					N20	3.042	141
					N21	2.640	169
	average	2.76	159	average		3.019	154

The active sites of SBP and PBP differ from one another in terms of their hydrogen bond networks.[10] Moreover, the presence of negative and positive charges in the PBP allows it to discriminate between phosphate and sulfate. The synthetic system, $\mathbf{6}H_2^{2+}$, bears two positively charged residues as mentioned above. Presumably as a consequence, both the sulfate and hydrogenphosphate anions are seen to form complexes in the solid state. Moreover, both anions are constrained within hydrogen bond networks that, while distinct (vide supra), are not all that different. However, these two tetrahedral anions are seen to bind with different affinities in acetonitrile solution and can thus be distinguished from one another (as well from other anions) under these ostensibly more exacting solution-phase conditions. This latter chemistry is summarized below.

Anion Binding Properties of Receptors 4−6. Although the crystal structures of **4** and **6**, both as reported earlier[9] and as discussed above, provided evidence that the protonated forms of macrocycles **4**−**6** are capable of interacting with anions in the solid state, it was considered important to probe their anion binding characteristics in solution. This had not been done previously, even in a preliminary fashion. However, several other smaller macrocycles were recently studied in acetonitrile.[17] Therefore, for the sake of consistency, and as dictated by solubility considerations, receptors **4**−**6** were analyzed for their ability to bind various inorganic anions in this same solvent system. As in our previous studies,[8,9,17] this was done by using standard UV−vis titrations employing the tetrabutylammonium (TBA) salts of the anions in question and the neutral forms of the receptors. The neutral (free base) forms were used in these studies, rather than one or more of the protonated forms, so as to avoid possible complications arising from incomplete protonation or counteranion effects (i.e., issues involving displacement equilibria).

Prior to carrying out the actual binding studies, the UV−vis spectra of **4** and **6** were recorded in acetonitrile. Interestingly, in spite of the strong chemical resemblance between receptors **4** and **6**, they were found to display slightly different spectra. In both cases, three maxima were seen, with those for **6** being shifted by 20−30 nm to longer wavelength (Figure 4). In the case of **4**, the central absorption maximum displays the highest intensity, whereas for **6** the three absorption maxima decrease in intensity with increasing wavelength. Of the various anions tested, only the hydrogensulfate anion was found to engender a significant change in color, with its addition to all three receptors serving to change the respective acetonitrile solutions from yellow to red. The addition of other anions does not serve to change the color of acetonitrile solutions of either **4** or **5**. However, the yellow color of the solution of **6** become more intense (brighter in aspect) upon the addition of excess chloride, phosphate, or nitrate (all three anions studied in the form of their respective tetrabutylammonium salts). These various changes are reflected in the corresponding titration curves (cf. Figure 4). For instance, the addition of hydrogensulfate anion induces an increase in the intensity of the bands at 520, 530, and 540 nm in the case of receptors **4**, **5**, and **6**, respectively, thereby giving rise to the observed red color. Likewise, the addition of dihydrogenphosphate anion to all three receptors induces an increase in the intensity at 425 nm with this increase being characterized by a significantly larger ΔA value in the case of **6**.

Interestingly, upon the addition of 1 equiv of $H_2PO_4^-$ to **6** the solution becomes slightly red (Figure 5). However, the continued addition of this anion causes the color to change back to yellow. This observation is considered to reflect the binding of more than one stoichiometric equivalent of dihydrogenphosphate anion to receptor **6**. In fact, the binding stoichiometry was determined to be 1:3 (receptor-to-anion) based on a Job plot analysis. Figure 4 shows the changes produced upon the addition of up to 1 equiv of $H_2PO_4^-$ and underscores the fact the same increase in the 540 nm band intensity is seen under these conditions as in the case of HSO_4^- titration. The similarity of the UV−vis spectra for receptor **6** seen after the addition of 1 equiv of either $H_2PO_4^-$ or HSO_4^- is rationalized in terms of the receptor folding around the anion to form a strong hydrogen bond network similar to that observed in the solid state.

As inferred from the UV−vis titrations, all of the receptors included in this study display a strong preference for the hydrogensulfate and dihydrogenphosphate anions in acetonitrile solution ($>10^4$ M^{-1} in all cases; approaching 10^7 M^{-1} in selected cases). In addition receptor **6** binds chloride and acetate anions strongly and even displays a propensity to bind large tetrahedral anions, such as perrhenate ($K_a \approx 10^3$ M^{-1}; Table 3). In contrast, receptor **4** was found to interact appreciably with only three of the current series of test anions, namely acetate, hydrogensulfate, and dihydrogenphosphate. Finally, receptor **5**, presumably as the result of containing more flexible methylamino linkers, can bind chloride anion. Although receptor **6** binds a number of anions well (i.e., with binding constants in the range 10^3−10^7 M^{-1}), it is the hydrogensulfate anion that displays the best combination of clean binding (i.e., 1:1 binding stoichiometry) and high affinity ($K_a \approx 10^7$ M^{-1}; Table 3). In contrast, dihydrogenphosphate is bound to this receptor well, albeit with a 1:3 receptor-to-anion stoichiometry, as noted above. Dihy-

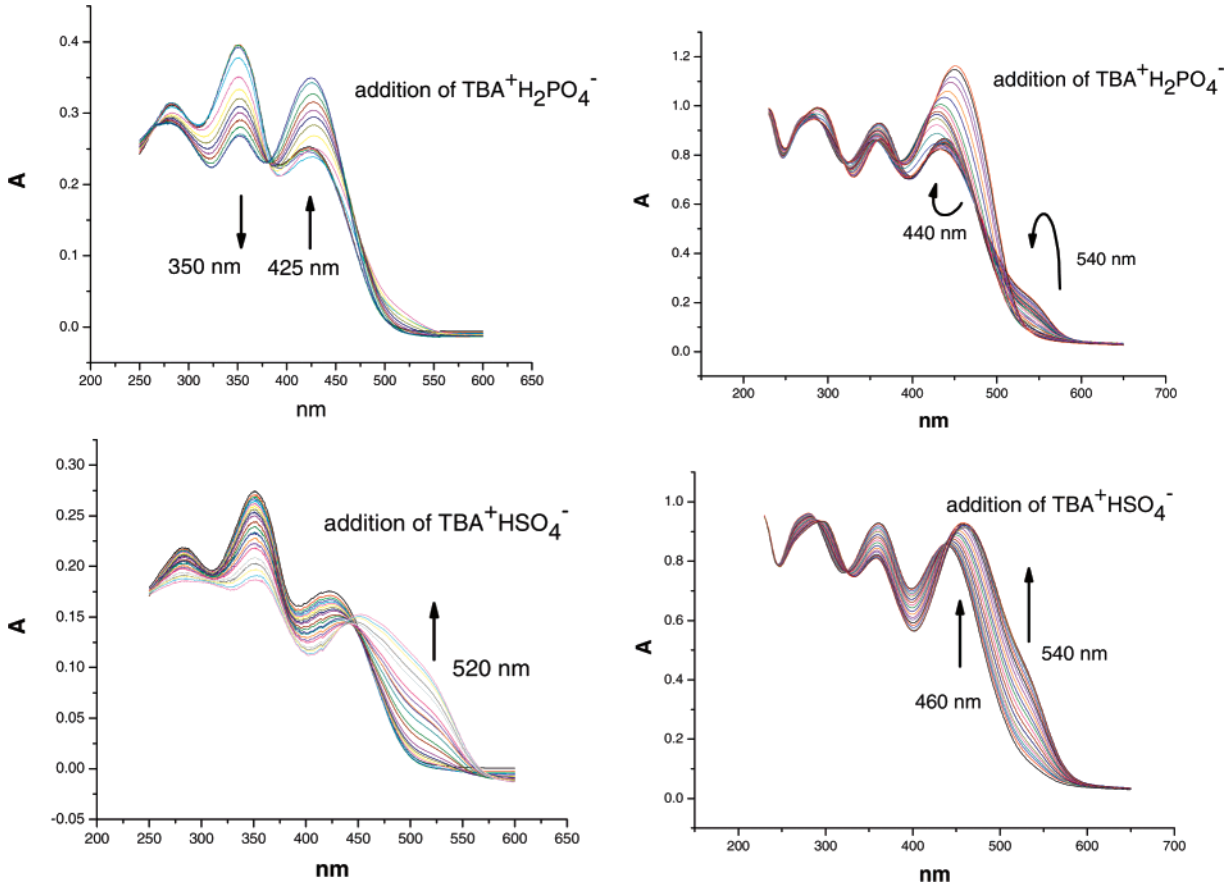

FIGURE 4. Changes in UV−vis spectra seen upon the addition of dihydrogenphosphate and hydrogensulfate to acetonitrile solutions of receptors **4** (left column) and **6** (right column).

FIGURE 5. Colors of acetonitrile solutions of receptor **6**: (1) free macrocycle, (2) with $TBA^+ Cl^-$, (3) with 1 equiv of $TBA^+ HSO_4^-$, (4) with 1 equiv of $TBA^+ H_2PO_4^-$, and (5) with ≥2 equiv of $TBA^+ H_2PO_4^-$.

drogenphosphate also binds to receptors **4** and **5** with a 1:2 stoichiometry.

The host−guest ratio for dihydrogenphosphate binding is seen to parallel the number of diiminobipyrrole subunits present in the receptor and, to the extent this inference is correct, the presence of amido-functional groups does not influence the binding of $H_2PO_4^-$. However, this conclusion does not hold for acetate and hydrogensulfate anions, where a higher relative affinity is observed for the pyridine-2,6-diamido containing macrocycle **4**. Moreover, for $H_2PO_4^-$ the association constant for **5** is almost identical with that of **4**, a finding that is consistent with the smaller macrocycle **4** being conformationally flexible. In other words, it appears, as expected, that it is not just the total number of interacting groups but also the way they are oriented to complement a given substrate (e.g., $H_2PO_4^-$) that is critical in terms of regulating both affinity and selectivity.

TABLE 3. Anion Affinities (log K_a) for the Interactions of Test Anions with the Bipyrrole-Derived Macrocyclic Receptors (Free Base Forms) 4−6, As Determined from UV−Vis Spectroscopic Titrations Carried out at 23 °C in Acetonitrile[d]

anion/ receptor	4	5	6
Cl^-	-[a]	3.385(7)	4.731(7)
Br^-	-[a]	-[a]	3.64(2)
NO_3^-	-[a]	-[a]	2.20(5)
CH_3COO^-	4.41(4)	3.38(3)	4.852(3)
ClO_4^-	-[a]	-[a]	3.57(8)[b]
ReO_4^-	-[a]	-[a]	3.35(8)[b]
HSO_4^-	4.80(3)	4.38(2)	6.99(1)
$H_2PO_4^-$[c]	5.28(3); 4.78(5)	5.78(2); 5.70(3)	6.74(6); 5.98(9); 4.11(6)

[a] No apparent binding seen, as reflected in the lack of observable change in the UV−vis spectrum upon anion addition. [b] Very weak changes in the UV−vis spectrum were observed over the course of the titration; this causes a relatively large error in derived binding constant. [c] Stepwise, 1:2 and 1:3 (receptor:anion) binding is observed; the values refer to those for the first, second, and third binding events, respectively. The numbers in parentheses are from the fits provided by the Hyperquad program; based on reproducibility, the actual experimental errors are considered to be ≤15%. All values in the table are the result of at least two independent experiments. [d] The corresponding tetrabutylammonium salts were used in all cases.

Conclusion

In this report we have detailed how large, bipyrrole-containing receptors may be made efficiently starting from appropriate

dialdehyde and diamine building blocks. This finding points the way toward the synthesis of receptors for different anionic species via the use of both appropriate starting materials and anionic templates. In the present instance, the starting materials **7**−**9** are readily available and are expected to arrange themselves around tetrahedral oxoanions, such as hydrogensulfate and dihydrogenphosphate, to form receptors **4**−**6** after imine bond formation. These receptors are selective for tetrabutylammonium hydrogensulfate and tetrabutylammonium dihydrogenphosphate, at least in acetonitrile solution. As inferred from UV−vis spectroscopic titrations, macrocycle **6** binds dihydrogenphosphate anion in a stepwise 1:3 binding in acetonitrile solution with a log K_a for the first binding event approaching 7. However, hydrogensulfate anion is bound with a 1:1 stoichiometry with a slightly higher affinity (log K_a even closer to 7). It is proposed that binding of 1 equiv of HSO_4^- or $H_2PO_4^-$ to **6** induces a conformational change that stabilizes an effective hydrogen bond network that bears analogy to that which is seen in the solid-state structure of the complex salt $\mathbf{6}H_2^{2+}\cdot HPO_4^{2-}$, as well as the active center of PBP. This congruence in terms of both structure and function leads us to suggest that receptors such as **6** could contribute to a further understanding of the factors that regulate anion binding in naturally occurring systems.

Experimental Section

Titration Conditions. Stock solutions of the host molecule subject to study were made up in acetonitrile, with the final concentrations being in the range of $1.3-1.7 \times 10^{-5}$ mol/L for **4**−**6**. Stock solutions of the guest were prepared by dissolving 15−25 equiv of the TBA salts of the anions in question in 5 or 10 mL of the host stock solution ($0-1 \times 10^{-3}$ mol/L). Making up the anion source solutions in this way allowed the binding studies to be carried out without having to make mathematical corrections to account for changes in host concentration as the result of dilution effects. The general procedure for the UV−vis binding studies involved making sequential additions of the titrant (anionic guest) to a 1 mL sample of the host stock solution in the spectrometric cell and monitoring the changes in the spectral features. The total number of data points was between 10 and 40, depending on the stoichiometry of complexation; for a presumed 1:1 complex 10−15 points were usually measured. The data points were then collated and combined to produce plots that, in turn, were processed by HYPERQUAD.[23]

X-ray Diffraction Analysis. X-ray experimental for $[C_{111}H_{113}N_{21}O_6]^{(2+)}[HPO_4]^{(2-)}$, $M_r = 1933.20$: Crystals grew as dark-red prisms and were obtained through the slow diffusion of pentane into a dichloromethane solution of the receptor. The data crystal was a prism that had approximate dimensions $0.24 \times 0.21 \times 0.18$ mm^3. The data were collected on a Bruker SMART 1000 CCD area detector diffractometer, using a graphite monochromator with Mo Kα radiation ($\lambda = 0.71073$ Å). A total of 81706 reflections were collected by using ω-scans with a scan range of 0.4 and a counting time of 40 s per frame. The data were collected at 120 K, using an Oxford Cryosystem low-temperature device. The crystal is triclinic, space group $P\bar{1}$, $a = 21.414(4)$ Å, $b = 23.166(4)$ Å, $c = 24.601(5)$ Å, $\alpha = 88.980(5)°$, $\beta = 78.128(5)°$, $\gamma = 84.935(5)°$, $Z = 4$, $V = 11896(4)$ Å^3, $\rho_{calc} = 1.079$ g/cm^3, $\mu = 0.084$ mm^{-1}, $\theta_{min} = 0.88°$, $\theta_{max} = 25.09°$. Data reduction was performed with SAINTPlus.[24] The structure was solved by direct methods and refined by full-matrix least-squares on F^2 with anisotropic displacement parameters for the non-H atoms. The hydrogen atoms on carbon were calculated in ideal positions with isotropic displacement parameters set to $1.2U_{eq}$ of the attached atom ($1.5U_{eq}$ for methyl hydrogen atoms). The hydrogen atoms bound to nitrogen atoms were observed in a ΔF map and refined with fixed position and isotropic displacement parameters. Six molecules of dichloromethane were found to be strongly disordered and could not be modeled satisfactorily. The contribution to the scattering by these molecules was removed by use of the utility SQUEEZE in PLATON98.[25] The function, $\sum w(|F_o|^2 - |F_c|^2)^2$, was minimized, where $w = 1/[(\sigma(F_o))^2 + (0.03P)^2]$ and $P = (|F_o|^2 + 2|F_c|^2)/3$. $R_w(F^2)$ refined to 0.1837, with $R(F)$ equal to 0.0996 and a goodness of fit, S, of 0.988. All calculations were carried out by use of the SHELXTL PLUS program (PC Version 5.10).[26]

Tetraamine 9 (2,6-dimethylamino(2-aminophenyl)pyridine). 2,6-Pyridinedialdehyde[27] (4 g, 29.60 mmol) and mono-BOC protected *o*-phenylenediamine (12.4 g, 59.5 mmol) were heated at reflux in 250 mL of MeOH for 2 h. The solution was cooled and product was filtered off. The solids collected in this way were then dissolved in a mixture of MeOH (200 mL) and CH_2Cl_2 (50 mL), after which $NaBH_4$ (1.44 g, 59.5 mmol) was added in small portions over 1 h. At this point, the solution was allowed to stir overnight at room temperature. It was then taken to dryness under reduced pressure. The resulting solid was redissolved in a mixture of CH_2Cl_2 (100 mL) and TFA (50 mL) and stirred for 2 h. The reaction mixture was then poured into 1 L of water containing 30 g of NaOH. After extraction with CH_2Cl_2, the organic phase was dried over $MgSO_4$. The resulting crude product was recrystallized from EtOAc−hexanes to give 5 g (53%) of **9** in the form of pale-yellow crystals. MS (CI^+, $M^+ + H$) *m*/*e* calcd for $C_{19}H_{22}N_5$ 320.4, found 320.2. Anal. Calcd for $C_{19}H_{21}N_5$: C, 71.45; H, 6.63; N, 21.93. Found: C, 71.11; H, 6.23; N, 21.80. ^{1}H NMR ($CDCl_3$) δ (ppm) 7.57 (t, 1H, $J = 7.6$), 7.20 (d, 2H, $J = 7.6$), 6.78−6.62 (m, 8H), 4.45 (s, 4H), 3.70 (br s, 4H). ^{13}C NMR ($CDCl_3$) δ (ppm) 157.8, 137.4, 137.2, 134.7, 134.3, 120.7, 120.2, 120.0, 118.8, 116.5, 112.2, 49.4.

Receptor 5. (Note: The full systematic name for this and other new products can be found in the Supporting Information.) 3,3′-Dimethyl-4,4′-dipropyl-5,5′-diformyl-2,2′-bipyrrole (**7**) (200 mg, 0.665 mmol) and 2,6-dimethylamino(2-aminophenyl)pyridine (**9**) (212 mg, 0.665 mmol) were mixed in 5 mL of methanol, after which 2 drops of concentrated H_3PO_4 (about 2.5 equiv) was added. The mixture was then stirred at rt for 48 h. The resulting dark red precipitate was filtered and washed with methanol to the receptor in the form of its phosphoric acid salt, $\mathbf{5}\cdot(H_3PO_4)_x$ ($x = 1-2$ according to elemental analysis). This salt was suspended in a mixture of dichloromethane and methanol at which point an excess of triethylamine was added. This addition caused the solution to turn bright yellow. After being taken to dryness in vacuo, the resulting solid was dissolved in dichloromethane and passed through a small alumina plug to yield 280 mg (72%) of the free receptor **5**. MS (ESI^+, M^+) *m*/*e* calcd for $C_{74}H_{82}N_{14}$ 1167.5, found 1168.4. Anal. Calcd for $C_{74}H_{82}N_{14}$: C, 76.13; H, 7.08; N, 16.80. Found: C, 76.00; H, 7.12; N, 16.80. ^{1}H NMR ($CDCl_3$) δ (ppm) 9.47 (br s, 4H), 7.27 (s, 2H), 7.14 (m, 4H), 7.02 (m, 4H), 6.95 (m, 4H), 6.63 (m, 4H), 6.60 (m, 4), 4.44 (m, 8H), 2.55 (m, 12H), 2.06 (s, 8H), 1.58 (m, 8H), 0.99 (t, $J = 12$ Hz, 12H). ^{13}C NMR ($CDCl_3$) δ (ppm) 158.5, 145.2, 142.9, 137.6, 137.1, 131.7, 128.1, 126.5, 125.7, 120.2, 119.4, 116.8, 116.3, 110.4, 49.3, 26.1, 24.7, 14.0, 10.2.

$6\cdot H_2SO_4$. The dihydrate of **4** (50 mg, 0.0408 mmol) prepared according to reference 9, was dissolved in 5 mL of CH_3CN at which point $TBAHSO_4$ (14 mg, 0.0412 mmol) was added. The solution was then left without stirring for 5 days before being layered with 50 mL of ether. The resulting precipitate was then filtered off and dried in vacuo to yield 25 mg (47%) of $\mathbf{6}\cdot H_2SO_4$ in the form of red

(23) Gans, P.; Sabatini, A.; Vacca, A. *Talanta* **1996**, *43*, 1739−1753.
(24) *SAINTPlus*, B; Bruker AXS: Madison, WI, 1998.
(25) Spek, A. L. In *PLATON, A Multipurpose Crystallographic Tool*; Utrecht University: Utrecht, The Netherlands, 1998.
(26) Sheldrick, G. M. In *SHELXTL*, v. 5.10, Structure Determination Software Suite; Bruker AXS: Madison, WI, 1998.
(27) Katayev, E. A.; Reshetova, M. D.; Ustynyuk, Y. A. *Russ. Chem. Bull. Int. Ed.* **2004**, *53*, 335−339.

crystals. MS (ESI^+, M^+) *m/e* calcd for $C_{111}H_{111}N_{21}O_6$ 1835.2, found 1835.0. Anal. Calcd for $C_{111}H_{113}N_{21}O_{10}S$: C, 68.96; H, 5.89; N, 15.21. Found: C, 68.93; H, 5.95; N, 15.20. ^1H NMR ($CDCl_3$) δ (ppm) 12.42 (s, 2H), 12.00 (m, 2H), 10.95 (s, 2H), 10.70 (s, 2H), 10.31 (s, 2H), 9.94 (s, 2H), 9.67 (s, 2H), 8.44 (t, $J = 8.4$ Hz, 4H), 8.40 (d, 2H), 8,13 (m, 3H), 8.02 (d, $J = 7.2$ Hz, 2H), 7.60 (d, $J = 7.8$ Hz, 2H), 7.45(m, 4H), 7.39 (m, 2H), 7.04 (m, 4H), 6.91 (m, 6H), 6.78 (m, 2H), 6.71 (d, $J = 7.2$ Hz, 2H), 6.50 (d, $J = 7.8$ Hz, 2H), 6.20 (m, 4H), 2.95 (m, 2), 2.60 (m, 4H), 2.14 (m, 6H), 1.99 (s, 6H), 1.80 (s, 14H), 1.65 (m, 5H), 1.51 (m, 5H), 1.26 (m, 5H), 1.00 (t, $J = 7.2$ Hz, 6H), 1.03 (t, $J = 7.2$ Hz, 6H), 0.49 (t, $J = 7.2$ Hz, 6H). ^{13}C NMR ($CDCl_3$) δ (ppm) 163.8, 161.1, 161.0, 150.7, 150.3, 150.2, 149.2, 148.9, 148.4, 146.6, 142.4, 138.8, 137.8, 137.1, 134.3, 132.8, 131.5, 130.7, 130.5, 129.5, 127.9, 127.5, 127.3, 127.2, 126.6, 125.9, 124.8, 124.7, 124.6, 124.6, 124.2, 123.8, 123.5, 122.8, 122.8, 121.6, 119.6, 119.6, 118.9, 118.7, 118.7, 118.2, 114.2, 99.9, 99.9, 98.3, 27.1, 26.6, 26.2, 24.8, 24.6, 22.9, 13.9, 13.9, 13.7, 13.2, 12.8, 12.4.

6·H_3PO_4. 3,3′-Dimethyl-4,4′-dipropyl-5,5′-diformyl-2,2′-bipyrrole[9] (**7**) (40 mg, 0.133 mmol) and bis(2-aminophenyl)pyridine-2,6-dicarboxamide (**8**) (42 mg, 0.144 mmol) were mixed in 1 mL of methanol after which 2 drops of concentrated H_3PO_4 (about 2.5 equiv) was added. The mixture was stirred for 48 h at rt. The resulting orange precipitate was filtered off and washed with methanol to yield 80 mg (46%) of the salt **6**·H_3PO_4. MS (ESI^+, M^+) *m/e* calcd for $C_{111}H_{111}N_{21}O_6$ 1835.2, found 1835.0. Anal. Calcd for $C_{111}H_{114}N_{21}O_{10}P$: C, 68.96; H, 5.94; N, 15.22. Found: C, 68.95; H, 5.87; N, 15.22. ^1H NMR ($CDCl_3$) δ (ppm), 14.30 (br s, 2H), 11.69 (br s, 2H), 10.62 (m, 5H), 10.36 (m, 2H), 8.49 (m, 2H), 8.37 (m, 4H), 8.06 (m, 5H), 7.64 (m, 4H), 7.47 (m, 2H), 7.37 (s, 2H), 7.09 (m, 2H), 7.01 (m, 2H), 6.84 (m, 7H), 6.70 (m, 4H), 6.49 (m, 2H), 6.04 (m, 4H), 2.94 (m, 2H), 2.62 (m, 4H), 2.24 (m, 3H), 2.08 (m, 4H), 2.03 (s, 6H), 1.93 (s, 6H), 1.90 (s, 6H), 1.64 (m, 5H), 1.55 (m, 4H), 1.24 (m, 5H), 1.03 (m, 12H), 0.49 (t, $J = 7.2$, 6H). ^{13}C NMR ($CDCl_3$) δ (ppm) 163.8, 160.9, 160.2, 152.1, 150.1, 149.5, 148.7, 148.5, 145.8, 143.7, 139.2, 138.8, 138.3, 137.6, 136.8, 136.4, 132.6, 131.5, 130.6, 130.4, 129.8, 127.9, 127.09, 126.8, 125.6, 124.9, 124.6, 124.5, 124.4, 124.1, 123.7, 123.2, 122.7, 122.2, 121.6, 119.9, 119.4, 118.5, 118.1, 114.3, 114.3, 99.9, 27.1, 26.9, 26.3, 24.9, 24.7, 22.8, 13.9, 13.9, 13.8, 13.6, 13.0, 12.6.

Receptor 6. Free receptor **6** was obtained from salt **6**·H_2SO_4 or **6**·H_3PO_4 by mixing it with an excess of triethylamine in dichloromethane, passing the resulting mixture through a small plug of silica gel, and evaporating the solution that elutes to dryness at rt.

Acknowledgment. This work was supported in part by the U.S. National Institutes of Health (grant no. GM 58907 to J.L.S.) and the Russian Foundation for basic research (grant nos. 05-03-32684 and 05-03-08017).

Supporting Information Available: Experimental part, UV−vis titrations curves, as well as X-ray crystallographic information including CIF files. This material is available free of charge via the Internet at http://pubs.acs.org.

JO071106G